**Proceedings of the ASME 2010 3rd Joint US-European Fluids Engineering Summer Meeting and 8th International Conference on Nanochannels, Microchannels, and Minichannels**
**FEDSM-ICNMM2010**
**August 1-5, 2010, Montreal, Canada**

# FEDSM-ICNMM2010-30531

# NUMERICAL INVESTIGATION OF THE EFFECT OF GEOMETRIC AND PHYSIOCHEMICAL PARAMETERS ON BIOMOLECULE CAPTURE EFFICIENCY

**Sina Jomeh**
University of British Columbia
Kelowna, BC, Canada

**Mina Hoorfar**
University of British Columbia
Kelowna, BC, Canada

## ABSTRACT

This paper presents and compares three different designs including open channel, circular pillar and screen-plate microreactors for capturing and detection of biomolecules in a buffer liquid. In general, these capturing/detection devices consist of a flow cell containing one or several reactive surfaces loaded with ligand molecules. The critical issue in the design of an efficient device is the proximity of the biomolecules to the ligands in the capturing stage since the latter is immobilized on the reactive surface and the former is freely moving in the flow. The flow pattern and the geometry of the device are the key factors in this regard. The presented designs are numerically modeled and compared in terms of capture efficiency. Immersed biomolecules are assumed to behave like a continuum medium. The Navier-Stokes and advection-diffusion equations are solved in two dimensions and the concentration profile is found after a certain sampling period. The chemical reaction between the ligand and the biomolecule is included in the model through solving the first order kinetic equation at the boundaries. The average surface concentrations of the adsorbed molecules are plotted and compared for all the geometries to determine the most efficient one. Considering the performance, ease of fabrication, and detection, the screen plates are found to be the best option for the purpose of biomolecule removal. The effects of the change in the geometric parameters (e.g., the flow path width in the microchannels) and physicochemical parameters (e.g., the diffusion constant, ligand surface density, and forward and backward reaction rates) involved in the problem on the adsorbed concentration are thoroughly inspected and the corresponding results are plotted.

## INTRODUCTION

Unique features of microfluidics devices have attracted researchers' interest in a wide range of disciplines including biochemistry and biotechnology. Due to their miniaturized design, different functionalities including mixing, pumping, separation and reaction can be integrated in narrow channels on a tiny chip. This helps to reduce the cost of mass production and the risk of contamination existing in conventional macroscale devices (1-3).

Microreactors are the essential constituent of microfabricated chips for many chemical and biotechnological applications. High surface-to-volume ratio (10000-50000 $m^2/m^3$) and fast rates of heat and mass transfer cause the reactions in such devices to be more efficient than the macroscale counterparts (4). The large value of the heat transfer coefficient leads to a more uniform sample temperature which itself results in a better control of experiment conditions. Moreover, the small size and the high rates intensify the reactions, shorten the residence time and consequently favor having higher throughputs (5).

One of the common applications of microreactors is to separate a phase from a buffer liquid using the binding specificity between two reactants. This idea, for instance, has been implemented in affinity chromatography to remove biological molecules from the liquid phase (6, 7). Surface plasmon resonance sensors (SPR) (8, 9), high frequency quartz microbalance (10) and hollow cantilever-based biosensors (11) used for adsorption kinetics studies are also among the examples of the above application. All the cases mentioned here deal with a buffer liquid flowing through a microchannel and mass being transported to the labelled surfaces.

Microreactors are generally divided into heterogeneous and homogenous categories. In homogeneous reactors, reaction takes place within the solution. Conversely, in heterogeneous reactors, one of the reactants (ligand) is immobilized on a solid surface and the other reactant is brought close to the surface by the carrier fluid. The reactive surface can be incorporated in thin layers on boundaries (so-called open channels) or in

packed-bed configurations within the flow domain (12). Because of the very small size and low Reynolds number, the main mechanism in open channels responsible for the transport of the immersed reactant is diffusion (13). Packed-bed designs help to add the effect of convection and decrease the diffusion path through constructing the reactive surfaces against the flow and reducing the size of flow passages (14). As a result, the capturing performance increases or alternatively, smaller chambers for the same throughput are fabricated.

In this paper, three different assemblies (open channel as well as packed-bed designs) of the reactive surfaces in a microchannel are studied. Each design is numerically modeled and compared with others in terms of the average surface concentration of the reactants. The first objective of this work is to investigate the effect of the reactive surface configuration on capturing efficiency. The first configuration considered here is a rectangular open channel. This design resembles the common flow chamber devices currently being used by the authors in their experimental setup for the study of hazardous microorganism detection inside drinking water. The next two designs are alternative configurations in packed-bed forms; one with circular pillars and the other one with screen plates. The numerical tool box introduced in this paper is developed to explore possible superiorities of one design with respect to the others. After finalizing the geometry, the next objective is to study the effect of other design parameters. These parameters range from chemical properties such as the ligand surface density and reaction rates to geometric properties like the distance between the plates or circles. The effects of these parameters are inspected and explained for the selected geometry by means of nondimensional numbers governing the problem of mass transport (15).

The paper is organized as follows: the geometries and dimensions are explained in detail in section 2. In section 3, the theory of mass and momentum transport are presented and the nondimensional numbers governing the problem are discussed. In section 4, the results are presented in two parts: the first part deals with finding the optimum configuration of the microreactor, and the second part investigates the parameters essential to the design process.

## NOMENCLATURE

| | |
|---|---|
| $C_b$ | biomolecule bulk concentration |
| $C_{b0}$ | biomolecule inlet bulk concentration |
| $C_s$ | biomolecule surface concentration |
| $C_{s0}$ | ligand surface concentration |
| $C_{s,ave}$ | average biomolecule surface concentration |
| $D$ | diffusion coefficient |
| $Da$ | Damkohler number |
| $K_D$ | equilibrium dissociation constant |
| $Pe$ | Peclet number |
| $h$ | flow path size |
| $k_{on}$ | forward reaction rate |
| $k_{off}$ | backward reaction rate |
| $l$ | length of the reactive surface |
| $\boldsymbol{n}$ | boundary normal vector |
| $p$ | pressure |
| $\boldsymbol{u}$ | velocity vector |
| $u_{ave}$ | average inlet velocity |
| $\varepsilon$ | relative adsorption capacity |
| $\mu$ | dynamic viscosity |
| $\rho$ | density |

## GEOMETRY

Figure 1 shows the microchannels with three different microreactor geometries considered for the analysis; a) parallel plates, b) circular micropillars, and c) screen plates. In all cases, the design criteria that the reactive surface area and the overall channel size must be the same are met. The width of the microchannel is 235 $\mu m$, and the height is 120 $\mu m$. The surface area of the reactor is considered 470 $\mu m^2$ for the screen-plate and parallel-plate designs (i.e., same as the reactive surface area currently implemented in the flow cell device used in the laboratory for the study of the hazardous microorganism detection inside drinking water). For the circular-micropillar design, the surface area is 471.2 $\mu m^2$ since in this case it is not possible to have exactly the same area as the others. Thus, an area very close to the set value (470 $\mu m^2$) is selected. The flow path in the circular-micropillar and screen-plate designs is 10 $\mu m$, which works well for biomolecules and small microorganisms without causing any clotting.

## THEORY

### Momentum Transport Equation

The buffer liquid is assumed to flow through a rectangular microchannel at steady state. Two-dimensional incompressible Navier-Stokes equations are used to find the velocity profile throughout the domain.

$$\rho \boldsymbol{u}.\boldsymbol{\nabla}\boldsymbol{u} = -\boldsymbol{\nabla}p + \mu\boldsymbol{\nabla}^2\boldsymbol{u} \quad (1)$$

The no-slip boundary condition is assumed at the walls.

### Mass Transport Equation

After the flow reaches the steady state, the solute (the immersed biomolecule) is released at the inlet at a specific concentration ($C_{b0}$), and its concentration is monitored over some sampling time period. This solute is carried by the liquid and transported to the reactive surfaces through diffusion and convection. The transient two-dimensional mass transport equation which is solved inside the domain is as follows:

$$\frac{\partial C_b}{\partial t} + \boldsymbol{u}.\boldsymbol{\nabla}C_b = D\boldsymbol{\nabla}^2 C_b \quad (2)$$

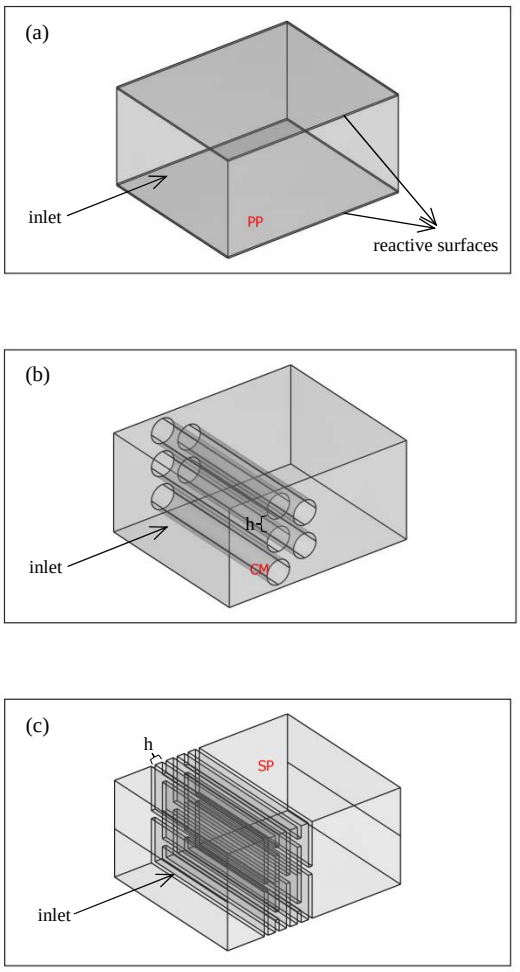


**Figure1. Geometries of three microreactors: a) open channel parallel plates (PP) in which top and bottom surfaces are reactive, b) circular micropillars (CM) in which cylinder surfaces are reactive and c) screen plates (SP) in which only front sides of the plates are reactive.**

where $C_b$ is the solute concentration in the bulk and $D$ is the diffusion coefficient.

For the chemical reaction at the reactive boundaries, rates of adsorption and desorption of the solute are included in the problem through a concentration flux term. The first-order kinetic equation of the chemical reaction is used to calculate this flux.

$$\frac{\partial C_s}{\partial t} = k_{on} C_{b,wall}(C_{s0} - C_s) - k_{off} C_s \tag{3}$$

$C_{s0}$ is the surface concentration of the ligand (the total number of free sites available for binding), $C_s$ is the surface concentration of the bound reactant (the number of occupied sites), $C_{b,wall}$ is the bulk concentration of the reactants close to the wall and $k_{on}$ and $k_{off}$ are forward and backward reaction rates, respectively.

At the outlet, the convective flux is specified as

$$\boldsymbol{n}.(-D\boldsymbol{\nabla} C_b) = 0 \tag{4}$$

in which $\boldsymbol{n}$ is the normal vector to the boundary. All other boundaries are insulated or symmetry, which means

$$\boldsymbol{n}.(-D\boldsymbol{\nabla} C_b + C_b\boldsymbol{u}) = 0 \tag{5}$$

## Non-dimensional Forms of the Governing Equations

Due to the diversity of the variables involved in the problem, nondimensionalizing is very helpful to understand the impact of each term on the output. This helps to explain the results in a more systematic way. The dimensionless forms of the mass transport and reaction kinetic equations are (15)

$$\frac{\partial C_b^*}{\partial t^*} + \left(u^* \frac{\partial C_b^*}{\partial x^*} + v^* \frac{\partial C_b^*}{\partial y^*}\right) = \frac{1}{Pe^2}\frac{\partial^2 C_b^*}{\partial x^{*2}} + \frac{\partial^2 C_b^*}{\partial y^{*2}} \tag{6}$$

$$\frac{\partial C_s^*}{\partial t^*} = \varepsilon Da[C_{b,wall}^*(1 - C_s^*) - K_D C_s^*] \tag{7}$$

where

$$x^* = \frac{x}{hPe}, y^* = \frac{y}{h}, t^* = \frac{Dt}{h^2}$$
$$u^* = \frac{u}{u_{ave}}, v^* = \frac{v}{u_{ave}}, C_b^* = \frac{C_b}{C_{b0}}, C_s^* = \frac{C_s}{C_{s0}}$$

$h$ is the characteristic length (e.g., channel height), $u_{ave}$ is the average inlet velocity, $Pe$ is Peclet number, $Da$ is Damkohler number, $\varepsilon$ is the relative adsorption capacity and $K_D$ is the equilibrium dissociation constant. Thus, the four main non-dimensional parameters governing the problem are

$$Pe = \frac{u_{ave}h}{D}, \varepsilon = \frac{C_{b0}h}{C_{s0}},$$
$$Da = \frac{k_{on}C_{s0}h}{D}, K_D = \frac{k_{off}}{k_{on}C_{b0}} \tag{8}$$

Peclet number is the ratio of the convection and diffusion strengths while Damkohler number is the relative strength of reaction at the surface and diffusion towards it. These numbers will be used later to interpret the behavior of the numerical results.

## RESULTS

### Capture Efficiency Comparison

Table 1 presents numerical values of the chemical and physical parameters observed in most biological reactions and used in the numerical solution (16-18). COMSOL Multiphysics software is used to solve the governing equations in two steps. First, the Navier-Stokes equations are solved in the domain and the steady-state velocity is found. Then, the mass transport equation is used along with the kinetic equation to derive the concentration profile of the solute in the bulk and on the surface. Throughout this paper, mesh independency is investigated with the margin of %1 change in the numerical results. The buffer liquid with the solute is allowed to flow through the channel for 5 minutes which is in the range of the usual sampling times. Due to symmetry, only half of each geometry is modeled.

Figures 2, 3 and 4 present concentration plots within the domain and on the reactive surfaces for each design. The average surface concentration deposited on the reactors is calculated using the following equation:

$$C_{s,ave} = \frac{1}{l} \int_{reactive\ area} C_s dx \qquad (9)$$

where, $l$ is the length of the reactive surface for unit depth of the channel. This concentration is used to compare the performance of each device. After five minutes, $C_{s,ave}$ is 0.321 $nmol/m^2$, 1.36 $nmol/m^2$ and 1.334 $nmol/m^2$ for parallel-plate, circular-micropillar and screen-plate designs, respectively. As it is expected, the performance significantly improves (4.2 fold increase) by changing the design from the open channel to the packed-bed geometry. This improvement is due to huge reduction in the diffusion path of the solute in the bulk and also, to some extent, the effect of convection. However, for the packed-bed designs, there is no significant achievement (within the numerical solution error) by using the screen plates instead of circular pillars. To compare the last two designs more accurately, the simulation is done for the same parameters but with twice the reactive surface used previously (results not shown here). It is obvious that increasing the reactive surface raises the surface concentration. But the average surface concentration is found to decrease for both cases. For the screen plates, the average surface concentration drops to 1.31 $nmol/m^2$ (about %1.8 decrease). For circular pillars the reduction is more, from 1.36 to 1.232 $nmol/m^2$ (by about %9.4). The circles in the downstream columns seem to be influenced a lot by the concentration wakes formed behind the circles in the upstream. With the circular design, it is also more difficult to keep the flow path size ($h$) close to 10 $\mu m$. Therefore, screen-plate design is more favorable especially when larger reactive surfaces, i.e. more columns, are required. In other words, screen plates seem to have better working performance in the range of the reactive surfaces used in the experiments. Moreover, plates greatly facilitate the process of fabrication and molecular detection for future studies. Based on the above discussion, the screen plate design is chosen as the best option.

**Table 1. Numerical values of parameters used for simulation**

| Parameter | Value |
|---|---|
| Forward reaction rate ($k_{on}$) | $10^5$ $m^3/(mol.s)$ |
| Backward reaction rate ($k_{off}$) | $10^{-2}$ $s^{-1}$ |
| Ligand concentration ($C_{s0}$) | $10^{-8}$ $mol/m^2$ |
| Diffusion coefficient (D) | $10^{-11}$ $m^2/s$ |
| Inlet concentration ($C_{b0}$) | $10^{-6}$ $mol/m^3$ |
| Average inlet velocity ($u_{ave}$) | $10^{-4}$ m/s |

### Analysis of the Screen-plate Design

This section investigates the influence of the chemical, physical and geometric design parameters on the output of the biomolecule separation process in the best design (i.e., the screen-plate design) selected in the previous section.

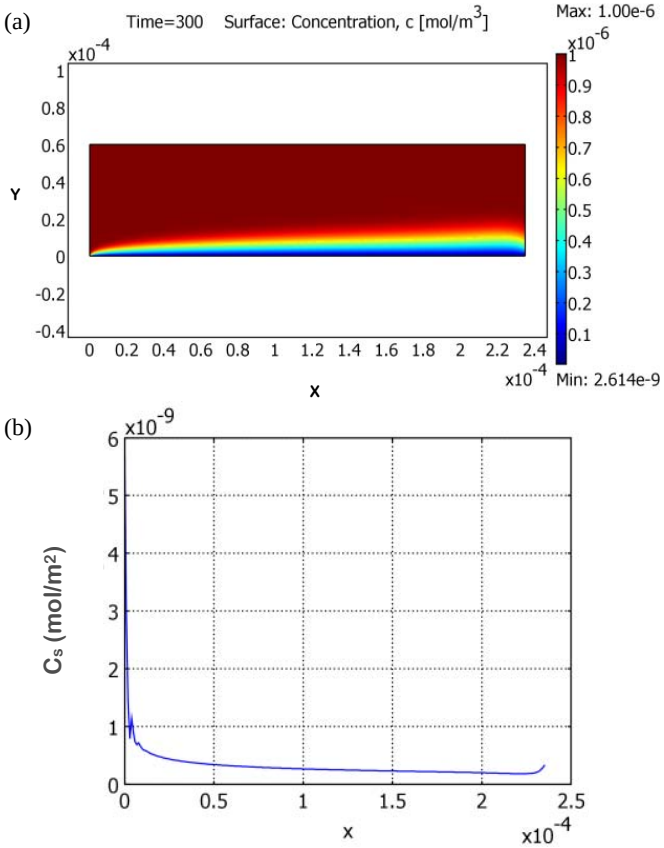


**Figure 2. Concentration plots (a) in the bulk, (b) on the reactive surface.**

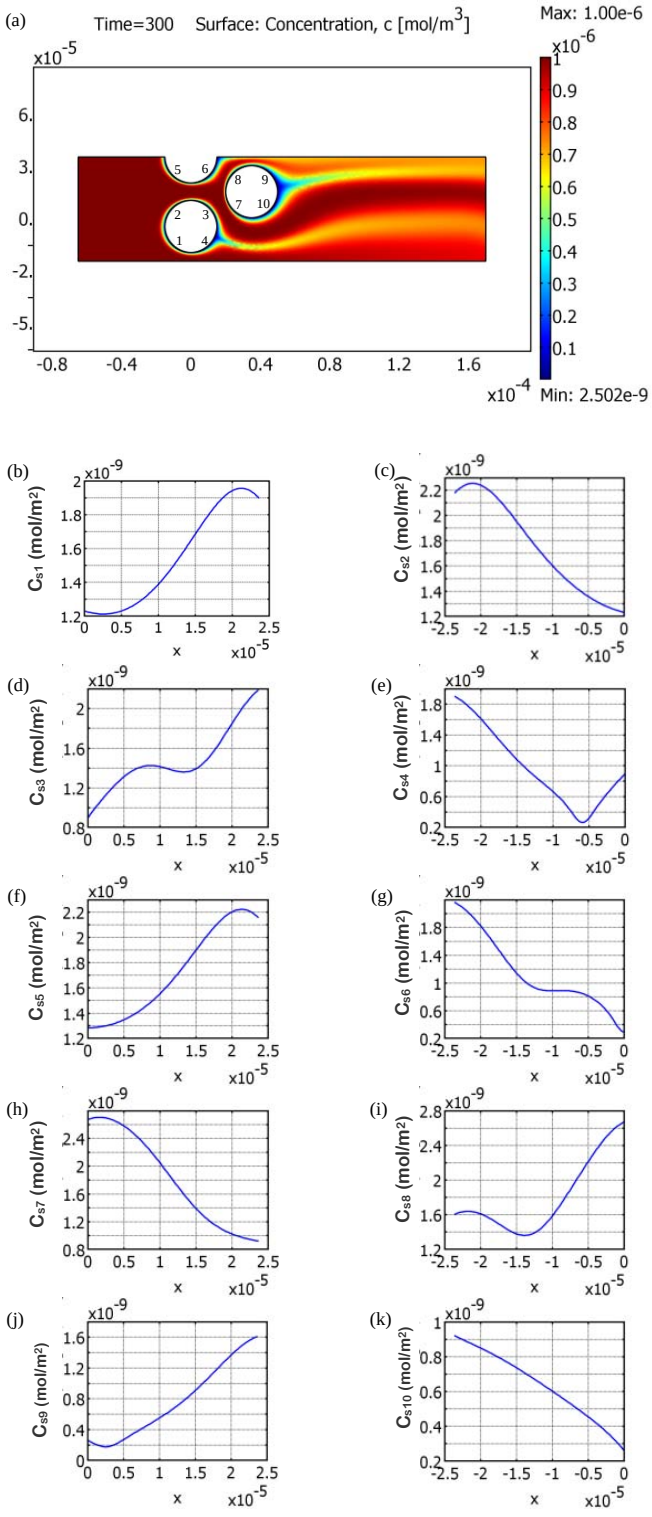


**Figure 3. Concentration plots (a) in the bulk, (b)-(k) on the reactive surfaces. Each reactive surface is a quarter of a circle numbered in Fig. 3a.**

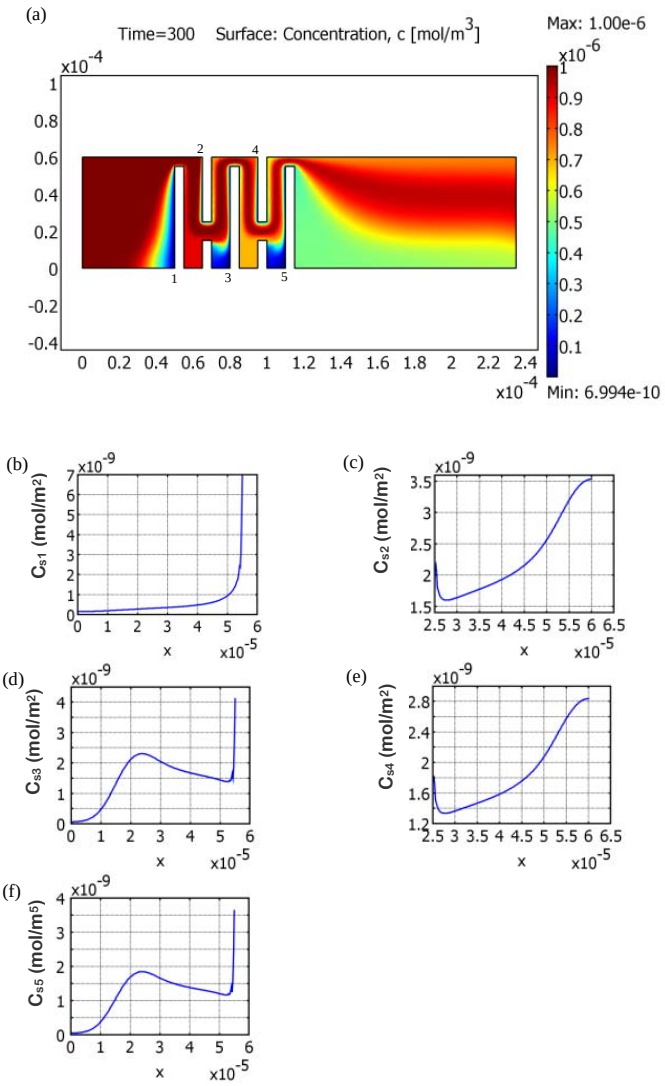


**Figure 4. Concentration plots (a) in the bulk, (b)-(f) on the reactive surfaces. Only front sides are reactive.**

***Forward and Backward Reaction Rates:*** Biomolecules differ in their affinity to bind to each other. Different types of ligands selected result in different values of the forward and backward reaction rates. As mentioned in Section 3.3, the forward reaction rate is included in two of the main four non-dimensional parameters of mass transport ( and ) while backward reaction rate is only presented in the dissociation constant ( ). Hence, it is expected that changing will have different effects on the average surface concentration than changing , even when the ratio of / is kept constant. That is why the forward and backward reaction rates are changed independently here. Figure 5 depicts the trend of the average surface concentration versus . As expected, augments when is increased. Five orders of magnitude change in gives almost one order of magnitude total change in . In semi-log plot, the curve has a deflection point

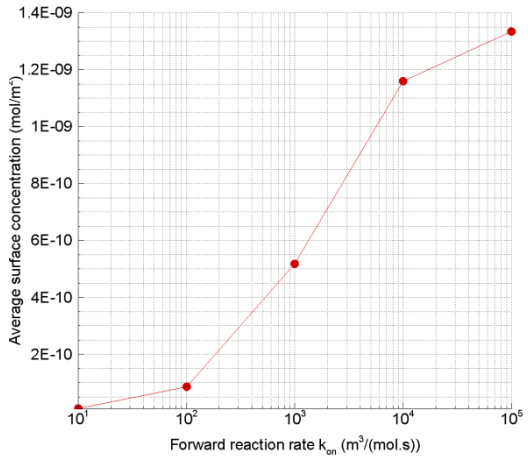


**Figure 5. Average surface concentration versus the forward reaction rate**

between $k_{on}$=$10^3$ and $10^4$ $m^3/(mol.s)$ up to which the gain in $C_{s,ave}$ is higher than when the experiment conditions lie after it (by the same change in $k_{on}$). This behaviour is also expected since for very high forward reaction rates, the transport-limited regime ($Da \rightarrow \infty$) is reached in which the surface concentration is limited by the transport process (15). It means further increase of $k_{on}$ will not have any significant influence on $C_{s,ave}$. Figure 6 reveals the similar trend for the change of $C_{s,ave}$ in terms of $k_{off}$ but in opposite direction; the higher the backward reaction rate, the lower the average surface concentration.

***Diffusion Coefficient:*** Biomolecules have different diffusivities in different solutions used for in-vitro experiments. Since the problem is very diffusion-dependent, a slight change in the diffusion coefficient, $D$, is expected to affect $C_{s,avg}$ significantly. Figure 7 shows the average surface concentration, $C_{s,avg}$, versus diffusion coefficient (which has been changed from $5\times10^{-12}$ to $3.2\times10^{-10}$ $m^2/s$).

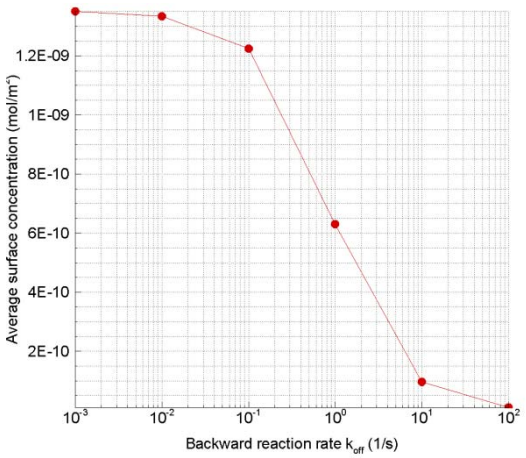


**Figure 6. Average surface concentration versus the backward reaction rate**

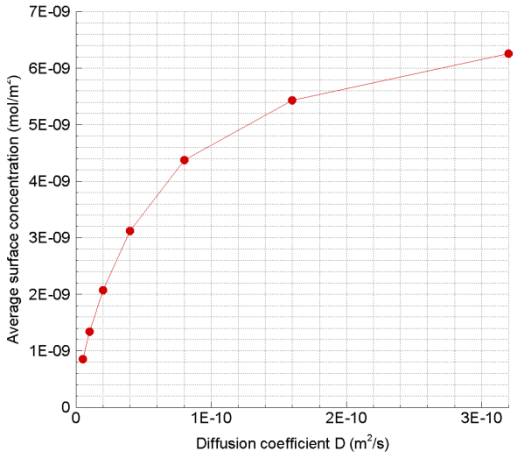


**Figure 7. Average surface concentration versus the diffusion coefficient**

At the beginning, the change is significant, but the rate decreases for larger values of $D$. This is due to the fact that increasing $D$ increases the $Da$ number until it is finite and the regime is changed to the reaction-limited one, where the adsorbed concentration is more a function of reaction parameters than diffusivity.

***Ligand Surface Concentration:*** The last physiochemical design parameter which is investigated here is the ligand surface concentration. Figure 8 presents the results. When $C_{s0}$ is doubled every time, the average surface concentration increases as the number of sites which have the potential for binding increases. However, this raises $Da$ number as well. It means that for larger $C_{s0}$, the regime is again being shifted to the transport-limited case, and $C_{s,avg}$ does not improve that much.

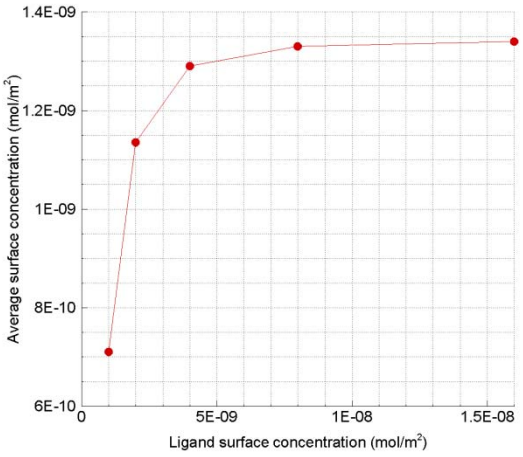


**Fig. 8. Average surface concentration versus ligand surface concentration**

***Distance between the Plates:*** Reorganizing the reactive surface and decreasing the diffusion path are the main factors responsible for enhancing the experiment throughput. In this section, the importance of this diffusion path is examined. Figure 9 plots the average surface concentration against the flow path size ($h$). In essence, the average concentration decreases when the flow area is wider, and this decrease becomes less significant when the size is very large. This proves that for higher values of $\boldsymbol{h}$, it takes longer for the reactants to transport to the surface. In the mean time, the reactants may be carried away by the flow (this is equivalent to having higher Peclet number).

## CONCLUSION

Microfluidics devices with flow-through channels and mass transport to reactive surfaces have gained lots of applications in recent chemical and biological research. The importance of a variety of the parameters governing the problem makes it very complicated to find the optimal configuration and range of working conditions to obtain the best result. In this paper, a numerical tool was introduced which enables the researcher to compare the performance of alternative assemblies of the same reactive area inside a fixed volume. Among the designs presented here, screen plates were proved to have the best performance for the range of reactive areas investigated. Although the difference in the performance of the screen-plate and circular-micropillar design is not considerable for smaller size of reactive surfaces, it becomes significant for larger number of plates and circles.

The numerical tool box also allows the thorough examination of the effect of physiochemical parameters on the device efficiency. Both mass transport-limited and reaction-limited regimes were observed in the plots when these parameters were changed over their usual ranges in biochemical reactions. Recognizing these regions can be useful to find out where the experiment conditions lie, and how to adjust them since some changes to the parameters do not significantly affect the output and are not worth the effort and the cost.

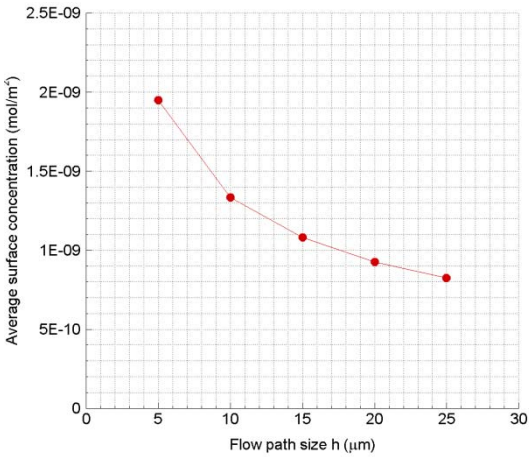


**Figure 9. Average surface concentration versus flow path size**

## REFERENCES


1. Chován, T., Guttman, A., 2002, "Microfabricated devices in biotechnology and biochemical processing," *TRENDS in Biotechnology*; *Vol. 20 (3)*, pp. 116-122.
2. Stone, H.A., Stroock, A.D., Ajdari, A., 2004, "ENGINEERING FLOWS IN SMALL DEVICES: Microfluidics Toward a Lab-on-a-Chip," *Annu. Rev. Fluid Mec.; Vol. 36*, pp. 381–411.
3. Whitesides, G. M., 2006, "The origins and the future of microfluidics," *Nature; Vol. 442*, pp. 368-373.
4. Kiwi-Minsker, L., Renken, A., 2005, "Microstructured reactors for catalytic reactions," *Catalysis Today; Vol. 110*, pp. 2–14.
5. Nguyen, N., Wereley, S.T., 2006, "Fundamentals and Applications of Microfluidics," ARTECH HOUSE, Norwood.
6. Hage, D.S., 1999, "Affinity Chromatography: A Review of Clinical Applications," *Clinical chemistry; Vol. 45 (5)*, pp. 593–615.
7. Snyder, L.R., Kirkland, J.J., Dolan, J. W., 2010, "Introduction to modern liquid chromatography," John Wiley & Sons. New Jersey.
8. Brockman, J.M., Nelson, B.P., Corn, R.M., 2000, "Surface Plasmon resonance imaging measurements of ultrathin organic films," *Annual Review of Physical Chemistry; Vol. 51*, pp. 41–63.
9. Schuck, P., 1997, "Use of surface plasmon resonance to probe the equilibrium and dynamic aspects of interactions between biological macromolecules," *Annual Review of Biophysics and Biomolecular Structure; Vol. 26*, pp. 541–566.
10. Okahata, Y., Kawase, M., Niikura, K., Ohtake, F., Furusawa, H., Ebara, Y., 1998, "Kinetic measurements of DNA hybridisation an oligonucleotide-immobilized 27-MHz quartz crystal microbalance." *Analytical Chemistry; Vol. 70 (7)*, pp. 1288–1296.
11. Burg, T.P., Manalis, S.R., 2003, "Suspended microchannel resonators for biomolecular detection," *Applied Physics Letters; Vol. 83 (13)*, pp. 2698–2700.
12. Oleschuk, R.D., Shultz-Lockyear, L.L., Ning, Y., Harrison, D.J., 2000, "Trapping of bead-based reagents within microfluidic systems: on-chip solid-

phase extraction and electrochromatography," *Analytical Chemistry; Vol. 72*, pp. 585-590.
13. Tabeling, P., 2005, "Introduction to Microfluidics," Oxford University Press, New York.
14. Berthier, J., Silberzan, P., 2006, "Microfluidics for biotechnology," Artech House, Norwood.
15. Gervais, T., Jensen, K.F., 2006, "Mass transport and surface reactions in microfluidic systems," *Chemical Engineering Science; Vol. 61*, pp. 1102 – 1121.
16. Hammer D.A., Lauffenburger, D.A., 1987, "A dynamical model for receptor-mediated cell adhesion to surfaces," *Biophysical Journal; Vol. 52*, pp. 475-487.
17. Bell G., Dembo M., Bongrand P., 1984, "Cell adhesion: competition between nonspecific repulsion and specific bonding" *Biophysical Journal; Vol.* 45, pp. 1051–1064.
18. Lawrence M. B., Springer T. A., 1991, "Leukocytes roll on a selectin at physiologic flow rates: distinction from and prerequisite for adhesion through integrins" *Cell; Vol 65*, pp. 859–873.